(Received 20 August 2025, Accepted 10 September 2025, Scheduled 22 September 2025)

Novel Designs of Quadrature 3-dB Impedance-Transforming Transdirectional Couplers Based on Double-Shielded Coupled Lines

Aleksandr N. Sychev*, Sergey A. Artishchev, Natalia S. Trufanova, and Nickolay Y. Rudyi

Department of Computer Systems
Tomsk State University of Control Systems and Radioelectronics (TUSUR), Tomsk 634050, Russia

ABSTRACT: Quadrature 3-dB impedance-transforming transdirectional (TRD) couplers based on double-shielded coupled lines are analyzed and synthesized; design relationships are also presented. To verify the proposed concept, two couplers implemented with high-permittivity (higher than 10) dielectrics are designed, fabricated, and measured. The first TRD coupler features a suspended ceramic bar, and the second one features a meandering layout of the upper line on a high-permittivity dielectric overlay. Comparison of the proposed solutions with known ones shows that novel coupler designs have advantages in small dimensions and an extended bandwidth of operating frequency (about 1.5–2 times). The simulated results are in good agreement with the measurement data.

1. INTRODUCTION

Directional couplers are a key component of a large number of microwave circuits. They are the basis for balanced amplifiers, mixers, attenuators, reflective phase shifters, beamforming networks, etc. Couplers based on coupled lines (CLs) are used especially widely (e.g., the Lange). There are three types of CL couplers: codirectional (COD), contra-directional (CTD), and transdirectional (TRD).

Note that COD and CTD couplers have been used for a long time, while CL-TRD coupler was proposed relatively recently in 2009, and was implemented by periodical shunt capacitors [1]. Subsequently, many modifications of CL-TRD couplers have been presented by other authors. DC isolated TRD coupler realized with multilayer liquid crystal polymer technology was considered as a component of phase shifters [2]. TRD coupler based on vertically installed planar (VIP) circuit without traditional lumped-elements (i.e., all-distributed) was proposed in [3]. Additionally, a filtering CL-TRD coupler with broadband bandpass response was presented in [4], and a miniaturized filtering TRD coupler with enhanced input-reflectionless feature was described in [5].

Besides, an arbitrary-phase-difference TRD coupler was proposed and applied in the design of a flexible Butler matrix [6]. A balun based on a power divider using TRD couplers in printed circuit board (PCB) technology was also implemented in [7]. All the above-described CL-TRD couplers had line-to-line symmetry, i.e., were built on symmetric CLs. At the same time, couplers of various types with impedance transformation properties are of great interest in microwave technology.

The first impedance-transforming coupler based on CLs was proposed by Cristal in 1966 [8], and it was a CTD coupler with synchronous waves. Later, many authors contributed to the development of CL-CTD couplers, including for the design of balanced amplifiers [9], etc. CL-CTD couplers were based on strongly asymmetric CLs, which were analyzed as two uncoupled two-wire transmission lines, which significantly simplified modelling and design procedure [10].

Impedance-transforming CL-TRD coupler with DC isolated input/outputs, which combines effects of impedance transformation and transverse directivity, was first introduced in 2023 [11]. Its creation became possible thanks to the use of double-shielded coupled lines (DSCLs) [12], also called strongly asymmetric CLs. The proposed design used a dielectric bar. Recently in 2024, an impedance-transforming CL-TRD coupler was also proposed, but it was realized only on low-permittivity dielectrics ($\varepsilon_r = 2.5$–3.4) [13]. Unfortunately, these couplers are large in size and have a narrow bandwidth.

To overcome these disadvantages, we propose original designs and implementations of the impedance-transforming TRD couplers based on DSCLs. They include a suspended ceramic bar and a meandering upper line on a high-permittivity overlay. These designs, using high-permittivity dielectrics, achieve impedance transformation, DC isolation, transverse directivity, wide bandwidth, and compact size.

The proposed impedance-transforming DSCL-TRD couplers can be used in the design of power dividers for balanced amplifiers, as in [9], replacing CL-CTD couplers, and in the design of hybrids to replace impedance-transforming branch-line couplers in reflection type phase shifters with a wide relative phase shift, as in [14], for phased-array antenna beamformers, etc.

* Corresponding author: Aleksandr N. Sychev (ans@main.tusur.ru).

2. MODELLING OF IMPEDANCE-TRANSFORMING DSCL-TRD COUPLER

2.1. Analysis of DSCLs

The scheme diagram of the impedance-transforming double-shielded coupled-line transdirectional (DSCL-TRD) coupler under study is shown in Fig. 1. Here, the first (upper) line is located inside the second (reference) line, which plays the role of an intermediate screen as shown in Fig. 2(a). To simplify the design, such DSCLs are implemented on the basis of multilayer structures with imperfect double shielding as shown in Figs. 2(b), (c), (d).

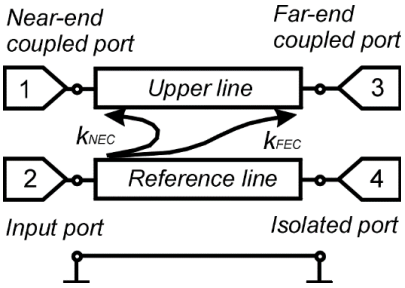

FIGURE 1. Schematic diagram of the impedance-transforming DSCL-TRD coupler.

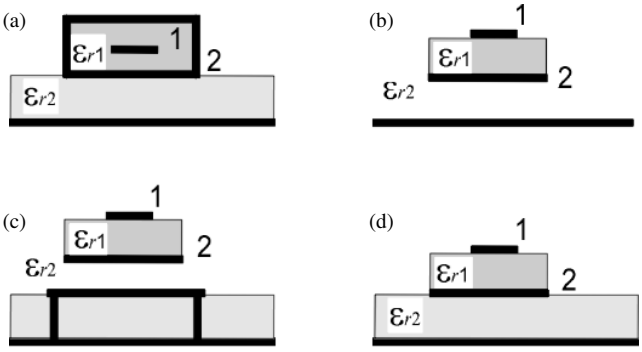

FIGURE 2. Cross sections of the DSCLs: (a) with perfect double shielding; (b), (c), and (d) with imperfect shielding.

Modeling of the DSCLs begins by solving the analysis problem. The equivalent circuit of the infinitely-short CL-section $\Delta x \to 0$ is shown in Fig. 3(a).

In quasi-static analysis, the primary parameters of the CLs are a pair of matrices: capacitances **C** and inductances **L** per unit length (PUL) [11, 12, 15]

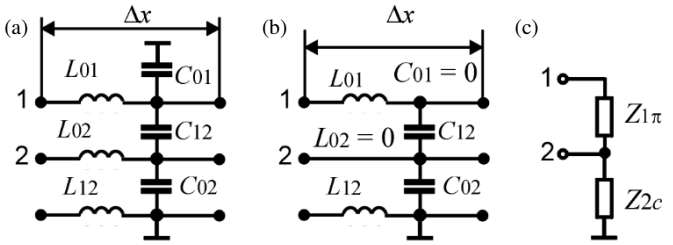

FIGURE 3. DSCL section: (a) equivalent circuit with length Δx; (b) when partial capacitance $C_{01} = 0$ and partial inductance $L_{02} = 0$; (c) as a lumped-element termination load.

$$\mathbf{C} = \begin{bmatrix} C_{11} & -C_{12} \\ -C_{12} & C_{22} \end{bmatrix} = \begin{bmatrix} C_{01}+C_{12} & -C_{12} \\ -C_{12} & C_{02}+C_{12} \end{bmatrix}$$
$$= \begin{bmatrix} C_{12} & -C_{12} \\ -C_{12} & C_{02}+C_{12} \end{bmatrix}_{C_{01}=0} \text{(F/m)} \quad (1)$$

$$\mathbf{L} = \begin{bmatrix} L_{11} & L_{12} \\ L_{12} & L_{22} \end{bmatrix} = \begin{bmatrix} L_{01}+L_{12} & L_{12} \\ L_{12} & L_{02}+L_{12} \end{bmatrix}$$
$$= \begin{bmatrix} L_{01}+L_{12} & L_{12} \\ L_{12} & L_{12} \end{bmatrix}_{L_{02}=0} \text{(H/m)} \quad (2)$$

where C_{11}, C_{22} are self-capacitances of the first and second lines; C_{01}, C_{02}, C_{12} are self-partial and mutual capacities, respectively; L_{11}, L_{22} are self-inductances of the first and second lines; L_{01}, L_{02}, L_{12} are self-partial and mutual inductances, respectively. Double shielding effect in CLs occurs when $C_{01} = 0$ and $L_{02} = 0$ [see Fig. 3(b)], so if CLs are perfect DSCLs, then $C_{11} = C_{12}$ and $L_{22} = L_{12}$.

Having determined the matrices of primary parameters **C** and **L**, we find their product, for which we then find the spectral decomposition by solving the algebraic eigenvalue problem, in which the found parameters are called modal parameters.

$$\mathbf{LC} = \frac{1}{c^2}\mathbf{U}\begin{bmatrix} \varepsilon_{rc} & 0 \\ 0 & \varepsilon_{r\pi} \end{bmatrix}\mathbf{U}^{-1} \quad (3)$$

where c is the speed of light in free space; ε_{rc} and $\varepsilon_{r\pi}$ are the modal effective permittivities of the CLs during in-phase (c-mode) and out-of-phase (π-mode) excitations, respectively; **U** is the modal voltage matrix composed of the eigenvectors of the **LC**-product matrix and is written as [11, 15, 16]

$$\mathbf{U} = \begin{bmatrix} 1 & 1 \\ R_c & R_\pi \end{bmatrix} = \begin{bmatrix} 1 & 1 \\ 1 & 0 \end{bmatrix}_{C_{01}=0}^{L_{02}=0} \quad (4)$$

where R_c, R_π are normalized modal voltages characterizing the voltage ratios on the lines, which in the case of perfect double shielding take the values $R_c = 1$ and $R_\pi = 0$, respectively.

Based on the obtained parameters, the modal current matrix **J** of the DSCLs is calculated, whose elements, as a result of the normalization, acquire units of admittance [11, 15]

$$\mathbf{J} = \mathbf{CU}\begin{bmatrix} c/\sqrt{\varepsilon_{rc}} & 0 \\ 0 & c/\sqrt{\varepsilon_{r\pi}} \end{bmatrix} = \begin{bmatrix} 0 & Z_{\pi 1}^{-1} \\ Z_{c2}^{-1} & -Z_{\pi 1}^{-1} \end{bmatrix}_{R_\pi=0}^{R_c=1} \quad (5)$$

where $Z_{\pi 1}$ and Z_{c2} are the π-mode-first-line impedance and the c-mode-second-line impedance, respectively [see Fig. 3(c)]. Further, using these matrices of modal voltages **U** and currents **J**, the matrix of characteristic impedances **Z** is found [15]

$$\mathbf{Z} = \mathbf{UJ}^{-1} = \begin{bmatrix} Z_{11} & Z_{12} \\ Z_{12} & Z_{22} \end{bmatrix}$$

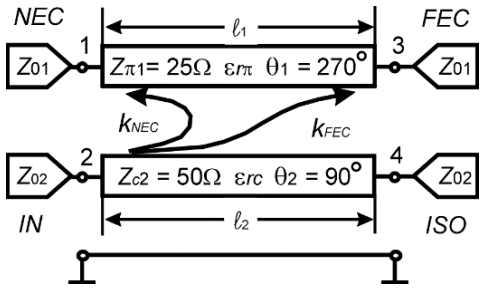

FIGURE 4. Schematic of the impedance-transforming DSCL-TRD coupler with different lengths of the upper ℓ_1 and reference ℓ_2 lines. In case if $\varepsilon_{r\pi}/\varepsilon_{rc} = 9$, then $\ell_1 = \ell_2$.

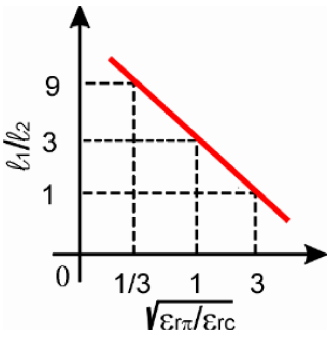

FIGURE 5. Geometric length ratio versus square root of effective permittivity ratio of the impedance-transforming DSCL-TRD coupler.

$$= \begin{bmatrix} Z_{\pi 1} + Z_{c2} & Z_{c2} \\ Z_{c2} & Z_{c2} \end{bmatrix}_{R_\pi = 0}^{R_c = 1} \tag{6}$$

which can be rewritten as follows

$$\mathbf{Z} = \frac{Z_0}{\sqrt{1-k^2}} \begin{bmatrix} 1/n & k \\ k & n \end{bmatrix} = \frac{Z_0}{\sqrt{1-k^2}} \begin{bmatrix} 1/k & k \\ k & k \end{bmatrix}_{R_\pi = 0}^{R_c = 1} \tag{7}$$

where Z_0 is the characteristic impedance; n and k are coefficients of the voltage transformation and impedance coupling, respectively. They are defined as follows

$$Z_0 = \sqrt{Z_{\pi 1} Z_{c2}};\ n = \sqrt{Z_{22}/Z_{11}};\ k = Z_{12}/\sqrt{Z_{11} Z_{22}}. \tag{8}$$

In case of the perfect double shielding, when $C_{01} = 0$; $C_{11} = C_{12}$, and $L_{02} = 0$; $L_{22} = L_{12}$, and $R_c = 1$; $R_\pi = 0$, the coupling coefficient k and voltage transformation ratio n of the DSCLs are equal to each other and are written as

$$n = k = \sqrt{\frac{Z_{c2}}{Z_{\pi 1} + Z_{c2}}} = \frac{1}{\sqrt{1 + Z_{\pi 1}/Z_{c2}}}. \tag{9}$$

2.2. Synthesis of Impedance-Transforming DSCL-TRD Coupler

As demonstrated in [11, 13], the TRD properties in the CLs coupler appear when the difference in modal electrical lengths is 180°. Therefore, an impedance-transforming DSCL-TRD coupler can be designed with two uncoupled two-wire transmission lines, one with 90° and the other with 270°, i.e.,

$$\theta_1/\theta_2 = 3; \quad \theta_1 - \theta_2 = \pi;$$

$$\frac{\theta_1}{\theta_2} = \frac{270^\circ}{90^\circ} = \frac{l_1\sqrt{\varepsilon_{r\pi}}}{l_2\sqrt{\varepsilon_{rc}}} = \begin{cases} \sqrt{\varepsilon_{r\pi}/\varepsilon_{rc}}, & l_1 = l_2; \\ l_1/l_2, & \varepsilon_{r\pi} = \varepsilon_{rc}. \end{cases} \tag{10}$$

where l_1, l_2 and θ_1, θ_2 are the geometric and electrical lengths of the upper (first) and reference (second) lines, respectively, as shown in Fig. 4. From (10) it is clear that if $\varepsilon_{r\pi}/\varepsilon_{rc} = 9$, then $l_1 = l_2$; and if $\varepsilon_{r\pi}/\varepsilon_{rc} = 1$, then $l_1 = 3l_2$. The relation between geometric length ratio and effective permittivity ratio in impedance-transforming DSCL-TRD coupler is shown in Fig. 5.

Note that the length of the upper line l_1 is expressed through the length of the reference line l_2 as follows

$$l_1 = k_{len} l_2 \tag{11}$$

where $k_{len} = 3/\sqrt{\varepsilon_{r\pi}/\varepsilon_{rc}}$ is the elongation factor.

Next, based on the theoretical analysis given above and in [11, 13], we can get synthesis formulas for the impedance-transforming DSCL-TRD coupler, taking into account a number of impedance conditions. Conditions for ideal isolation, perfect impedance matching, and nominal couplings at the central frequency of the DSCL-TRD coupler (see Fig. 4) are as follows

$$R = Z_{02}/Z_{01} = 1/k_{\text{NEC}}^2, \tag{12}$$

$$Q = \sqrt{R-1} = k_{\text{FEC}}/k_{\text{NEC}}, \tag{13}$$

$$k_{\text{NEC}}^2 + k_{\text{FEC}}^2 = 1; \tag{14}$$

$$\frac{Z_{01}}{Z_{02}} = k_{\text{NEC}}^2; \quad \frac{Z_{\pi 1}}{Z_{c2}} = k_{\text{FEC}}^2; \tag{15}$$

$$\frac{Z_{\pi 1}}{Z_{01}} = \frac{k_{\text{FEC}}}{k_{\text{NEC}}} = Q; \quad \frac{Z_{c2}}{Z_{02}} = \frac{k_{\text{NEC}}}{k_{\text{FEC}}} = \frac{1}{Q}. \tag{16}$$

$$\frac{Z_{\pi 1}}{Z_{c2}} = \frac{Z_{01}}{Z_{02}} Q^2; \tag{17}$$

$$Z_0^2 = Z_{01} Z_{02} = Z_{\pi 1} Z_{c2}; \tag{18}$$

$$\begin{cases} Z_{\pi 1} = Z_{01} Q; \\ Z_{c2} = Z_{02}/Q. \end{cases} \tag{19}$$

where Z_{01}, Z_{02} are termination impedances of the upper (first) and reference (second) lines, respectively; R is the impedance transformation ratio; k_{NEC}, k_{FEC} are nominal coefficients of the near-end and far-end coupling, respectively, of the loaded impedance-transforming DSCL-TRD coupler.

The coupling coefficient k and voltage transformation ratio n of the DSCL-section are written as

$$n = \sqrt{\frac{1 + k_{\text{FEC}}^2 R_\pi^2}{R_c^{-2} + k_{\text{FEC}}^2}}; \quad k = \frac{n + R_c R_\pi / n}{R_c + R_\pi}. \tag{20}$$

In the case of perfect shielding, i.e., in ideal DSCLs, when $C_{01} = 0$; $L_{02} = 0$, and $R_c = 1$; $R_\pi = 0$, we get equality between n and k, as given above in (9)

$$n = k = \frac{1}{\sqrt{1 + k_{\text{FEC}}^2}} = \frac{1}{\sqrt{2 - k_{\text{NEC}}^2}} \Bigg| \begin{array}{l} R_c = 1 \\ R_\pi = 0 \end{array}. \quad (21)$$

As a result of the synthesis procedure, the matrices of capacitances **C** and inductances **L** PUL of the DSCLs are written as follows

$$d = 1/(R_c - R_\pi); \quad (22)$$

$$\begin{cases} z_1 = \sqrt{\varepsilon_{r\pi}} Z_{\pi 1}; \\ z_2 = \sqrt{\varepsilon_{rc}} Z_{c2}; \end{cases} \quad \begin{cases} y_1 = \sqrt{\varepsilon_{r\pi}}/Z_{\pi 1}; \\ y_2 = \sqrt{\varepsilon_{rc}}/Z_{c2}; \end{cases} \quad (23)$$

$$\mathbf{L} = \frac{d}{c} \begin{bmatrix} z_1 R_c + z_2/R_c & z_1 R_c R_\pi + z_2 \\ z_1 R_c R_\pi + z_2 & z_1 R_c R_\pi^2 + z_2 R_c \end{bmatrix}$$

$$= \frac{1}{c} \begin{bmatrix} z_1 + z_2 & z_2 \\ z_2 & z_2 \end{bmatrix}_{L_{02}=0} (\text{H/m}); \quad (24)$$

$$\mathbf{C} = \frac{d}{c} \begin{bmatrix} y_1 R_c + y_2 R_c R_\pi^2 & -(y_1 + y_2 R_c R_\pi) \\ -(y_1 + y_2 R_c R_\pi) & y_1/R_c + y_2 R_c \end{bmatrix}$$

$$= \frac{1}{c} \begin{bmatrix} y_1 & -y_1 \\ -y_1 & y_1 + y_2 \end{bmatrix}_{C_{01}=0} (\text{F/m}), \quad (25)$$

where c is the speed of light in free space.

From these relations, we again find that in the case of perfect double shielding ($C_{01} = 0$; $L_{02} = 0$; $R_c = 1$; $R_\pi = 0$), two coupled lines can be considered as two uncoupled lines with impedances of $Z_{\pi 1}$ and Z_{c2}, and effective permittivities $\varepsilon_{r\pi}$ and ε_{rc}, respectively, as shown early in [13]. However, the analysis can be carried out in the case of imperfect shielding [11].

It should also be noted that by definition (see Fig. 1 and Fig. 4) the electrical length of the reference line of the impedance-transforming DSCL-TRD coupler (i.e., the section length) is equal to 90 degrees at the center frequency.

2.3. Ideal Impedance-Transforming DSCL-TRD Coupler

As a numerical example of the presented model, we consider an ideal impedance-transforming DSCL-TRD coupler in the case of perfect double shielding.

1) Let the system impedance $Z_{02} = 50\,\Omega$, the nominal coupling at the center frequency NEC $= 3$ dB, and the modal effective permittivities $\varepsilon_{rc} = 2$; $\varepsilon_{r\pi} = 18$, and then using (10)–(25), we obtain

$$\begin{cases} k_{\text{NEC}} = 10^{-\text{NEC}/20} = 1/\sqrt{2} = 0.707; \\ k_{\text{FEC}} = \sqrt{1 - k_{\text{NEC}}^2} = 1/\sqrt{2} = 0.707; \end{cases}$$

$$Z_{01} = Z_{02} k_{\text{NEC}}^2 = 25\,\Omega.$$

2) The impedance transformation ratio of the 3-dB DSCL-TRD coupler is determined by the nominal coupling coefficient k_{NEC} and equals 2.

$$R = Z_{02}/Z_{01} = 1/k_{\text{NEC}}^2 = 2.$$

3) Other impedance parameters are calculated as follows

$$Q = \sqrt{R - 1} = k_{\text{FEC}}/k_{\text{NEC}} = 1;$$

$$\begin{cases} Z_{\pi 1} = Z_{01} Q = 25\,\Omega; \\ Z_{c2} = Z_{02}/Q = 50\,\Omega; \end{cases}$$

$$Z_0 = \sqrt{Z_{\pi 1} Z_{c2}} = 35.4\,\Omega.$$

4) The coupling coefficient k and voltage transformation ratio n of ideal DSCLs are equal to each other and are calculated as in (21)

$$n = k = \frac{1}{\sqrt{1 + k_{\text{FEC}}^2}} = \frac{1}{\sqrt{2 - k_{\text{NEC}}^2}} = \sqrt{2/3} = 0.816.$$

5) The matrix of characteristic impedances **Z** is calculated

$$\mathbf{Z} = \begin{bmatrix} Z_{\pi 1} + Z_{c2} & Z_{c2} \\ Z_{c2} & Z_{c2} \end{bmatrix} = \begin{bmatrix} 75 & 50 \\ 50 & 50 \end{bmatrix} \Omega.$$

6) The matrices of capacitances **C** and inductances **L** PUL are also calculated in (24) and (25)

$$\mathbf{L} = \frac{1}{c} \begin{bmatrix} z_1 + z_2 & z_2 \\ z_2 & z_2 \end{bmatrix}_{L_{02}=0} = \begin{bmatrix} 0.589 & 0.236 \\ 0.236 & 0.236 \end{bmatrix} \left(\frac{\mu\text{H}}{\text{m}}\right);$$

$$\mathbf{C} = \frac{1}{c} \begin{bmatrix} y_1 & -y_1 \\ -y_1 & y_1 + y_2 \end{bmatrix}_{C_{01}=0} = \begin{bmatrix} 566 & -566 \\ -566 & 660 \end{bmatrix} \left(\frac{\text{pF}}{\text{m}}\right).$$

3. EXPERIMENTAL RESULTS

Using theoretical model and design relationships, two 3-dB impedance-transforming TRD couplers based on DSCLs are proposed and designed with high-permittivity dielectrics. The first TRD coupler has a feature in suspended ceramic bar with $\varepsilon_r = 20$, and the second TRD coupler features a meandering layout of the upper line on a dielectric overlay with $\varepsilon_r = 10$.

3.1. Impedance-Transforming DSCL-TRD Coupler with Suspended Ceramic Bar

The schematic diagram, geometry, and photograph of 3-dB impedance-transforming DSCL-TRD coupler-1 with suspended ceramic bar and two additional $\lambda/4$-length impedance transformers are shown in Fig. 6, Fig. 7, and Fig. 8, respectively.

This TRD coupler is fabricated on a 1-mm thick dielectric substrate FLAN-10 ($\varepsilon_r = 10$, from Factory "Moldavizolit", Tiraspol, Transdnistrian Moldavian Republic) and has following physical parameters: $(w_1, w_2, h_1, h_2, h, t, \ell) = (1, 2, 0.5, 0.51, 1, 0.02, 28)$ mm

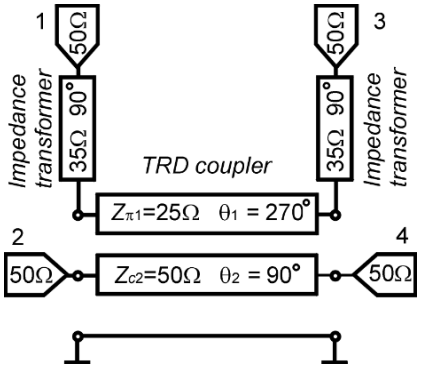

FIGURE 6. Schematic diagram of 3-dB impedance-transforming DSCL-TRD coupler with suspended ceramic bar and two additional $\lambda/4$-length impedance transform.

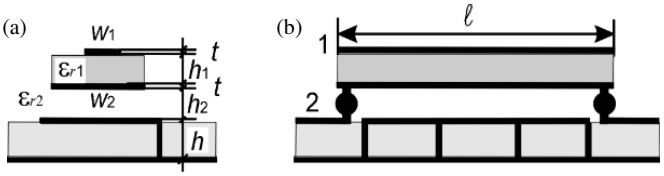

FIGURE 7. Geometry of 3-dB impedance-transforming DSCL-TRD coupler with suspended ceramic bar: (a) cross-sectional view; (b) side view.

$(\varepsilon_{r1}, \varepsilon_{r2}) = (20, 1)$, as shown in Fig. 7. The ceramic bar (V20 from "Ceramics" Ltd., Saint Petersburg, Russia) of rectangular cross-section 0.5 by 2 mm with broadside-coupled striplines is elevated above the top metal plate, which is connected to the bottom ground plane through four via holes [see Fig. 7(b), Fig. 8]. The conductive strips on the ceramic bar are made from silver-containing paste using plotter [17].

Calculated using the conformal mapping technique [18] and implemented in the original Lines Modelling Toolbox CAD, primary parameters of the DSCLs are $(L_{11}, L_{22}, L_{12}) = (0.407, 0.193, 0.146)$ μH/m, $(C_{11}, C_{22}, C_{12}) = (478, 522, 469)$ pF/m.

Corresponding modal parameters are $(Z_{\pi 1}, Z_{c2}) = (21.5, 64.1)\,\Omega$ and $(R_c, R_\pi, \varepsilon_{rc}, \varepsilon_{r\pi}) = (1, -0.181, 1.04, 13)$. Note that because the shielding is not perfect ($R_\pi \neq 0$), we need all six parameters because four is not enough.

For measurement purposes, additional quarter-wavelength impedance transformers are connected to the near- and far-end coupled ports of the coupler, as shown in Fig. 6 and Fig. 8.

They are realized as microstrip line sections of 1.8 mm wide and 12 mm long ($Z_T = 35.4\,\Omega$; $\theta = 90°$). The fabricated coupler has been measured with vector network analyzer Planar S5048.

Simulated and measured S-parameters of the impedance-transforming DSCL-TRD coupler with suspended ceramic bar are shown in Fig. 9 and Fig. 10. Simulated operating frequency band is (1.92–2.54) GHz, i.e., 27% at the central frequency 2.2 GHz. The amplitude imbalance is (3.3 ± 0.6) dB, isolation (insertion loss) of the upper line and return loss of reference line more than 20 dB, isolation (insertion loss) of the reference line and return loss of the upper line more than 10 dB.

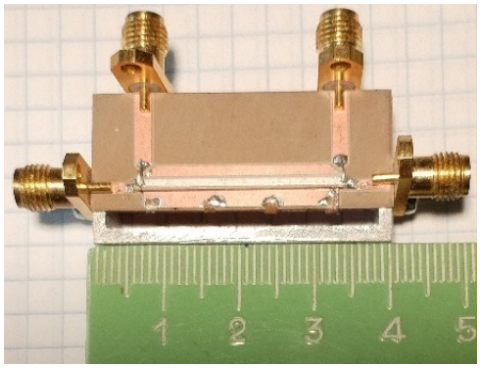

FIGURE 8. Photograph of 3-dB impedance-transforming DSCL-TRD coupler with suspended ceramic bar and two additional $\lambda/4$-length impedance transformers.

Measured results show that the operating frequency band is 1.75–2.25 GHz, i.e., 25% at the central frequency 2 GHz. The amplitude imbalance is 3.5 ± 1.5 dB; phase imbalance is 92 ± 2 deg; isolation of the upper line and return loss of reference line is more than 20 dB; isolation of the reference line and return loss of the upper line is more than 10 dB. The error in calculating the center frequency and operating frequency band do not exceed 10%.

3.2. Impedance-Transforming DSCL-TRD Coupler with Upper Meander Line

Schematic diagram, geometry, and photograph of 3-dB impedance-transforming DSCL-TRD coupler-2 with upper meander line and two additional L-section matching networks are shown in Fig. 11, Fig. 12, and Fig. 13, respectively.

This TRD coupler is fabricated on a 1.5-mm thick dielectric substrate FR-4 ($\varepsilon_r = 4.9$) as PCB (12×25 mm) and has following physical parameters: $(w_1, w_2, h_1, h_2, t, \ell_1, \ell_2) = (0.8, 2.5, 0.254, 1.5, 0.035, 33, 16.5)$ mm; $(\varepsilon_{r1}, \varepsilon_{r2}) = (10.2, 4.9)$, as shown in Fig. 12. Upper line with a meandering layout is located on the dielectric overlay ($\varepsilon_r = 10.2$, RO3010 from Rogers Co.) of the TRD coupler [see Fig. 12(c)]. The calculated modal parameters of the DSCLs are $(Z_{\pi 1}, Z_{c2}) = (24, 52)\,\Omega$; $(R_c, R_\pi, \varepsilon_{rc}, \varepsilon_{r\pi}) = (1, -0.1, 3.6, 7.3)$.

For measurement purposes, additional L-section matching networks are connected to the near- and far-end coupled ports of the TRD coupler, as shown in Fig. 11 and Fig. 13. Each of them consists of a shunt capacitor ($C = 1.0$ pF), realized with a foil plate measuring 4 by 8.5 mm, and a series inductor ($L = 1.6$ nH), made of a copper wire 2.5 mm long and 0.25 mm in diameter.

Simulated and measured S-parameters of the impedance-transforming DSCL-TRD coupler with upper meander line are shown in Fig. 14 and Fig. 15. Simulated operating frequency band is 2.18–2.8 GHz, i.e., 25% at the central frequency 2.5 GHz. The amplitude imbalance is (3.8 ± 1.2) dB; isolation of the upper line and return loss of the reference line is more than 20 dB; isolation of the reference line and return loss of the upper line is more than 10 dB.

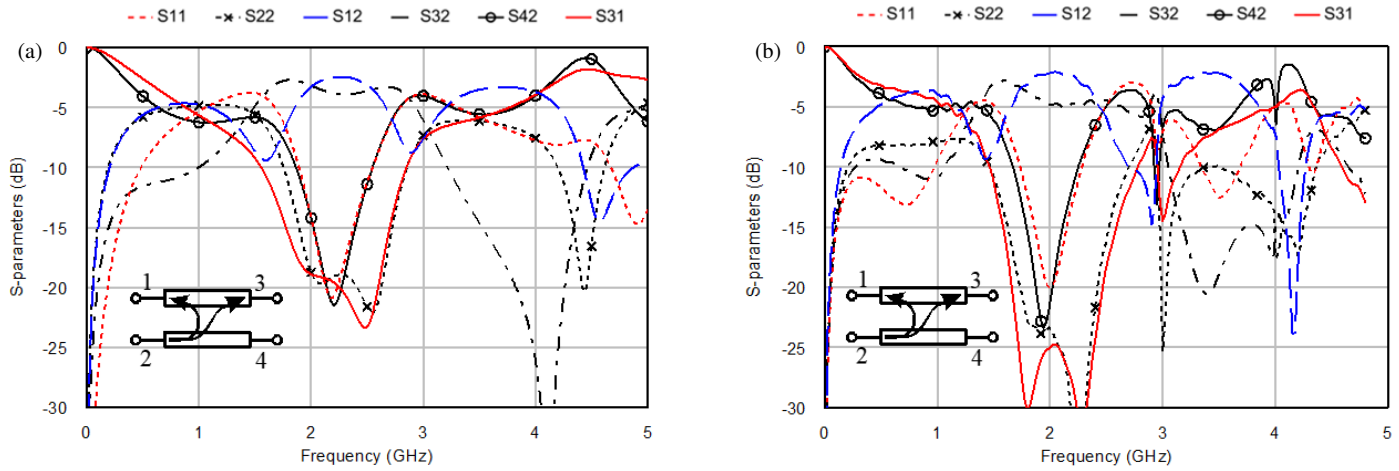

FIGURE 9. (a) Simulated and (b) measured S-parameters of 3-dB impedance-transforming DSCL-TRD coupler with suspended ceramic bar.

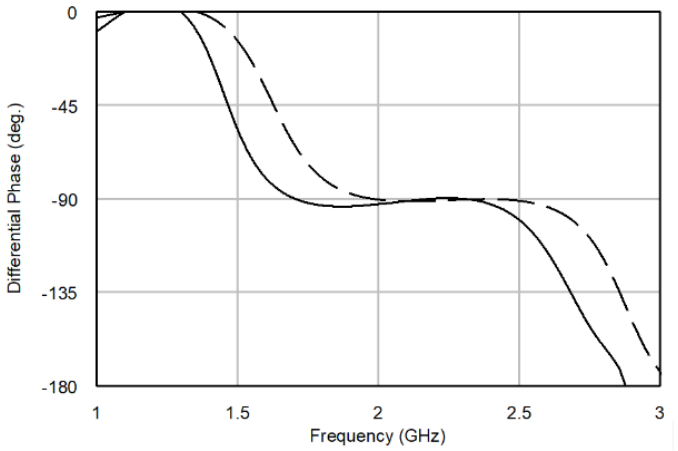

FIGURE 10. Simulated (dashed) and measured (solid line) phase differences between 1 and 3 ports of 3-dB impedance-transforming DSCL-TRD coupler with suspended ceramic bar.

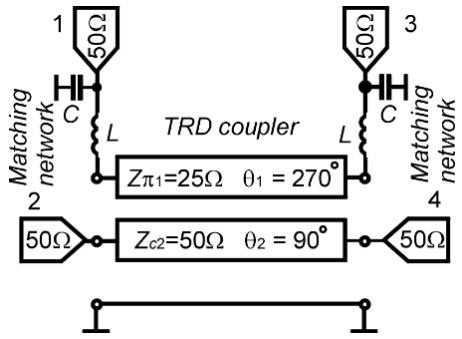

FIGURE 11. Schematic diagram of 3-dB impedance-transforming DSCL-TRD coupler with upper meander line and two additional L-section matching networks.

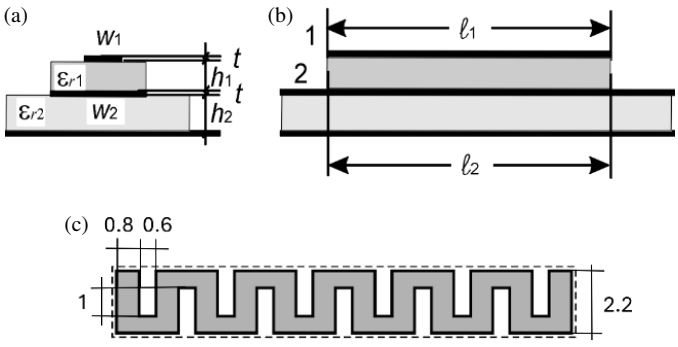

FIGURE 12. Geometry of 3-dB impedance-transforming DSCL-TRD coupler with upper meander line: (a) cross-sectional view; (b) side view; and (c) top view of the meander line.

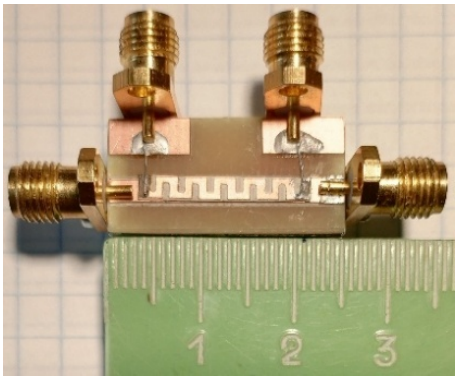

FIGURE 13. Photograph of 3-dB impedance-transforming DSCL-TRD coupler with upper meander line and two additional L-section matching networks.

Measured results show that the operating frequency band is 2.4–3.0 GHz, i.e., 22% at the central frequency 2.7 GHz. The amplitude imbalance is (4 ± 1) dB; phase imbalance is (89 ± 4) deg; isolation of the upper line and return loss of the reference line is more than 20 dB; isolation of the reference line and return loss of the upper line is more than 10 dB. The error in calculating the center frequency does not exceed 8%.

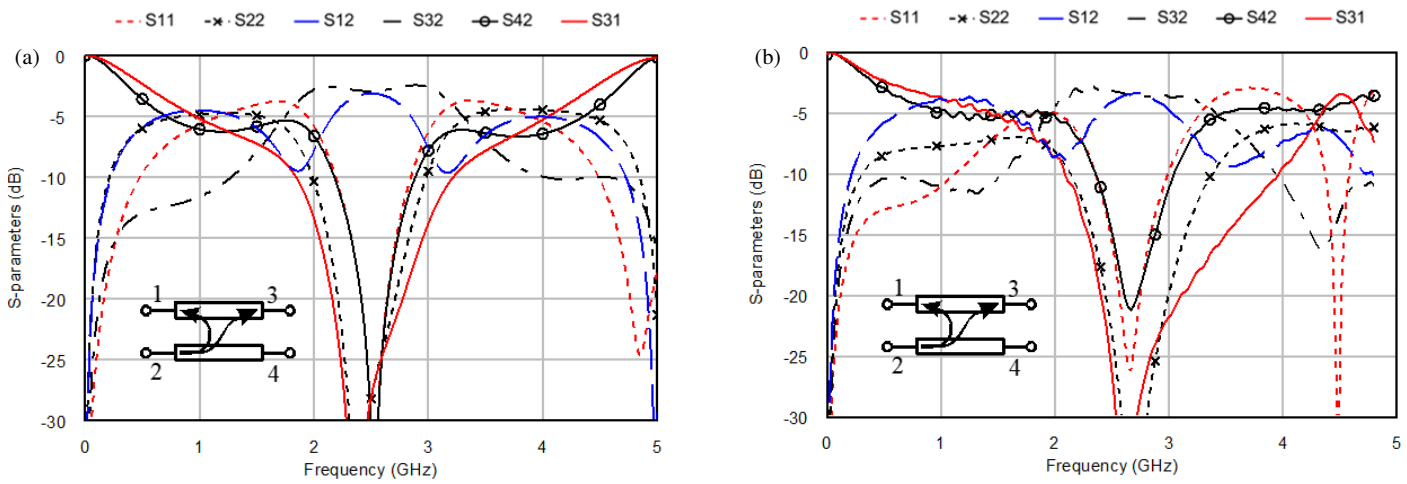

FIGURE 14. (a) Simulated and (b) measured S-parameters of 3-dB impedance-transforming DSCL-TRD coupler with upper meander line.

TABLE 1. State-of-the-art of the quadrature 3-dB impedance-transforming CL CTD and TRD couplers.

Ref.	[1]	[10]	[19]*	[11]	[13]	**This work**	**This work**
Type of quadrature directional CL coupler	TRD	CTD	TRD	TRD	TRD	**TRD-1**	**TRD-2**
DC-isolated input/outputs	yes	no	yes	yes	yes	**yes**	**yes**
Center frequency (GHz)	3.6	1.0	1.8	1.85	1.0	**2.0**	**2.7**
Bandwidth (%)	22	n/a	29	18	12	**25**	**22**
Amplitude balance (dB)	3**±1	3**±n/a	3**±1	3.7±0.7	3**±n/a	**3.5±1.5**	**4±1**
Phase balance (deg.)	90±5	90±n/a	100±15	90±n/a	90±n/a	**92±2**	**89±4**
Impedance transformation ratio $R = Z_{02}/Z_{01}$	1	2	1.5	2	2	**2**	**2**
Scheme and terminal impedances (Ω)	Fig.16 (a)	Fig.16 (b)	Fig.16 (c)	Fig.16 (d)	Fig.16 (d)	Fig.16 (d)	Fig.16 (d)
Number of coupled sections	1	1	10	1	1	**1**	**1**
Design	microstrip	coaxial/ microstrip	microstrip	multilayer [see Fig. 2 (b)]	multilayer	**multilayer [see Fig. 2 (c)]**	**multilayer [see Fig. 2 (d)]**
Dielectric constant ratio $\varepsilon_{r1}/\varepsilon_{r2}$ (see Fig. 2)	-	-	-	16/1	3.38/2.5	**20/1**	**10.2/4.9**
Layout of the upper line	straight	straight	straight	straight	meander	**straight**	**meander**
Section length (mm)	12 (0.14 λ)	45 (0.15 λ)	10.2 (0.06 λ)	33 (0.2 λ)	50 (0.17 λ)	**28 (0.19 λ)**	**16.5 (0.15 λ)**

* Because of the difficulties of assembly of smaller capacitors, this 3-dB TRD coupler is not fabricated; only calculated values are given here.
** Nominal coupling value.
λ: wavelength at the center frequency.

4. DISCUSSION

A comparison of features of known 3-dB impedance-transforming CL CTD/TRD couplers with the proposed designs is given in Table 1. In this table, the first CL-TRD coupler has DC-isolated input/outputs, but does not have impedance transformation function as shown in Fig. 16(a) [1]. In the second CL-CTD coupler, one conductor is shielded from the other and combines the contra-directional property with impedance transformation as shown in Fig. 16(b) [10]; however, it does not have the transdirectional property.

Other CL-TRD couplers shown in Table 1 and Fig. 16(c), although they are transdirectional, differ significantly from the others in that they do not provide impedance equality at the ends of one of the lines, which limits the area of its application, and due to the complexity of the design, they remained physically unrealized [19].

Let us note that impedance-transforming DSCL-TRD coupler combines the effects of impedance transformation and transverse directivity. In addition, a unique property of the TRD coupler is the galvanic isolation between the input port and a pair of output ports located at the near and far ends of the coupled line (see Fig. 1). This feature cannot be achieved in the known CTD solutions described in [10]. Therefore, only [11] and [13] (see Table 1) present impedance-transforming DSCL-TRD couplers and have the schematic diagram shown in Fig. 16(d), similar to that in Fig. 1. However, unlike them, the proposed 3-dB impedance-transforming TRD couplers based on DSCLs are designed with high-permittivity dielectrics.

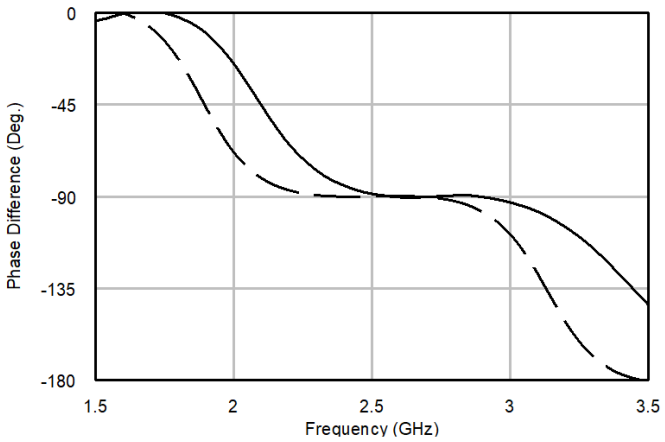

FIGURE 15. Simulated (dashed line) and measured (solid line) phase differences between ports 1 and 3 of 3-dB impedance-transforming DSCL-TRD coupler with upper meander line.

The first TRD-1 coupler has a feature in suspended ceramic bar with $\varepsilon_r = 20$, and the second TRD-2 coupler features a meandering layout of the upper line on a dielectric overlay with $\varepsilon_r = 10$. So unlike [13], where dielectrics with only low permittivity ($\varepsilon_r = 2.5$–3.4) are applied, the proposed DSCL-TRD coupler designs use an upper dielectric with high permittivity ($\varepsilon_r = 10$–20), which allows the ceramic bars and overlays to be mounted as conventional SMD components and reducing the dimensions of the couplers. Hence, the main advantages of the proposed designs, in contrast to known [11] and [13], are small dimensions and an extended bandwidth of operating frequencies (about 1.5–2 times).

5. CONCLUSION

Novel quadrature hybrids in the form of 3-dB impedance-transforming DSCL-TRD couplers, which combine the effects of impedance transformation and transverse directivity, are investigated. The presented analysis of DSCLs, in the case of perfect double shielding, when $C_{01} = 0$, $L_{02} = 0$, $R_c = 1$, $R_\pi = 0$, shows that the coupling coefficient k and voltage transformation ratio n of the DSCLs are equal to each other, which simplifies the modeling.

A matched 3-dB impedance-transforming DSCL-TRD coupler has a double impedances ratio ($Z_{02}/Z_{01} = Z_{c2}/Z_{\pi 1} = 50/25$) and a triple electrical lengths ratio ($\theta_1/\theta_2 = 270/90$). The triple ratio of electrical lengths can be achieved either by the geometric lengths ratio, or by the dielectric permittivities ratio, or by a combination of both. All these techniques have been employed to develop new designs. Two 3-dB impedance-transforming DSCL-TRD couplers are implemented with high-permittivity dielectrics. The first TRD coupler features a suspended ceramic bar with $\varepsilon_r = 20$, and the second one features a meandering layout of the upper line on a dielectric overlay with $\varepsilon_r = 10$.

The key advantages of the proposed quadrature 3-dB impedance-transforming DSCL-TRD couplers are DC-isolated input/outputs, a compact size, and an extended operating bandwidth.

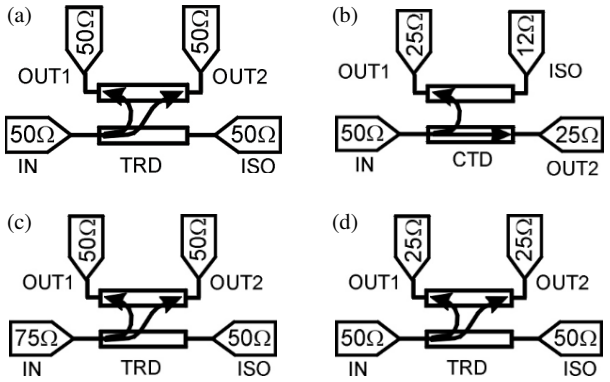

FIGURE 16. Schematic diagrams of the quadrature 3-dB impedance-transforming CL CTD and TRD couplers with their terminal impedances.

ACKNOWLEDGEMENT

This work was supported by the Russian Science Foundation under Grant No. 25-29-00316, https://rscf.ru/en/project/25-29-00316/.

REFERENCES

[1] Shie, C.-I., J.-C. Cheng, S.-C. Chou, and Y.-C. Chiang, "Transdirectional coupled-line couplers implemented by periodical shunt capacitors," *IEEE Transactions on Microwave Theory and Techniques*, Vol. 57, No. 12, 2981–2988, Dec. 2009.

[2] Turalchuk, P., I. Munina, I. Vendik, J. Ni, and J. Hong, "DC isolated directional coupler," in *2014 44th European Microwave Conference*, 93–95, Rome, Italy, 2014.

[3] Sychev, A. N., S. M. Struchkov, V. N. Putilov, and N. Y. Rudyi, "A novel trans-directional coupler based on vertically installed planar circuit," in *2015 European Microwave Conference (EuMC)*, 283–286, Paris, France, 2015.

[4] Liu, H., X. Li, Y. Guo, S.-J. Fang, and Z. Wang, "Design of filtering coupled-line trans-directional coupler with broadband bandpass response," *Progress In Electromagnetics Research M*, Vol. 100, 163–173, 2021.

[5] Zhang, Y., Y. Wu, and W. Wang, "Miniaturized filtering trans-directional coupler with enhanced input-reflectionless feature using two types of coupled multi-line sections," *International Journal of RF and Microwave Computer-Aided Engineering*, Vol. 32, No. 12, e23427, 2022.

[6] Liu, H., S. Fang, Z. Wang, and S. Fu, "Design of arbitrary-phase-difference transdirectional coupler and its application to a flexible Butler matrix," *IEEE Transactions on Microwave Theory and Techniques*, Vol. 67, No. 10, 4175–4185, Oct. 2019.

[7] Jeannin, L., L. Boukhezar, O. Occello, L. Vincent, G. Ducournau, M. L. Roy, A. Pérennec, and P. Ferrari, "A versatile balun based on a power divider topology," in *2024 54th European Microwave Conference (EuMC)*, 3–6, Paris, France, 2024.

[8] Cristal, E. G., "Coupled-transmission-line directional couplers with coupled lines of unequal characteristic impedances," *IEEE Transactions on Microwave Theory and Techniques*, Vol. 14, No. 7, 337–346, Jul. 1966.

[9] Wincza, K. and S. Gruszczynski, "Asymmetric coupled-line directional couplers as impedance transformers in balanced and N-way power amplifiers," *IEEE Transactions on Microwave Theory and Techniques*, Vol. 59, No. 7, 1803–1810, Jul. 2011.

[10] Wincza, K., S. Gruszczynski, and S. Kuta, "Approach to the design of asymmetric coupled-line directional couplers with the maximum achievable impedance-transformation ratio," *IEEE Transactions on Microwave Theory and Techniques*, Vol. 60, No. 5, 1218–1225, May 2012.

[11] Sychev, A. N., V. A. Bondar, K. B.-B. Dagba, A. I. Stepanyuga, and N. Y. Rudyi, "Theory of doubly-shielded coupled lines for directional couplers of various directivity types with impedance transformation," *IEEE Transactions on Microwave Theory and Techniques*, Vol. 71, No. 5, 2104–2117, May 2023.

[12] Matsumoto, A., *Microwave Filters and Circuits*, 349, Academic Press, New York, London, 1970.

[13] Wincza, K., K. Staszek, R. Smolarz, and S. Gruszczynski, "Impedance-transforming transdirectional coupled-line directional couplers with maximum achievable transformation ratio," *IEEE Access*, Vol. 12, 93 841–93 847, 2024.

[14] Lin, C.-S., S.-F. Chang, C.-C. Chang, and Y.-H. Shu, "Design of a reflection-type phase shifter with wide relative phase shift and constant insertion loss," *IEEE Transactions on Microwave Theory and Techniques*, Vol. 55, No. 9, 1862–1868, Sep. 2007.

[15] Tripathi, V. K., "Asymmetric coupled transmission lines in an inhomogeneous medium," *IEEE Transactions on Microwave Theory and Techniques*, Vol. 23, No. 9, 734–739, Sep. 1975.

[16] Sychev, A. N., "Synthesis of modal and distributed parameters of asymmetric coupled lines with inhomogeneous dielectrics," *Journal of Radio Electronics*, No. 6, 2024.

[17] Trufanova, N. S., S. A. Artishchev, A. G. Loschilov, and E. R. Ragimov, "Manufacturing of hybrid integrated circuits using additive printer technology," in *2022 International Siberian Conference on Control and Communications (SIBCON)*, 1–5, Tomsk, Russia, 2022.

[18] Sychev, A. N. and K. K. Zharov, "Analysis of asymmetric broadside coupled lines by conformal mapping technique," in *2019 International Siberian Conference on Control and Communications (SIBCON)*, 1–3, Tomsk, Russia, 2019.

[19] Oraizi, H. and M. J. Siahkari, "Optimum design of multi-section asymmetrical transdirectional couplers with port impedance matching up to S band frequency," *International Journal of Antennas and Propagation*, Vol. 2022, No. 1, 4046706, 2022.